



Experimental study on the evaporation heat transfer characteristics of R-1234yf with a variation in tube diameter

Sung-Hoon Seol¹ · Jeong-In Yoon² · Joon-Hyuk Lee³ · Han-Som Jeong⁴ · Soo-Jeong Ha[†]

(Received July 28, 2021 ; Revised August 12, 2021 ; Accepted August 18, 2021)

Abstract: Freon-based refrigerants, which are excellent in terms of efficiency and stability, have a high global warming potential; therefore, Hydrofluoroolefin(HFO)-based refrigerants are attracting interest as alternative refrigerants for refrigeration and air-conditioning systems. In particular, R-1234yf, which has similar thermal properties to R-134a but has less impact on the environment, is being considered as an alternative refrigerant. Therefore, in this study, an experimental study on evaporation heat transfer characteristics was conducted using R-1234yf in horizontal tubes with inner diameters of 3.7, 5.3, and 6.8 mm. The evaporation heat transfer characteristics were identified at a saturation temperature of 5–15 °C, mass flux of 200–500 kg/m²s, heat flux of 5–15 kW/m², and quality of 0–1. The effects of changes in quality, mass flux, heat flux, saturation temperature, and tube diameter on the evaporation heat transfer coefficient were revealed, and the evaporation heat transfer coefficients of R-1234yf and R-134a were compared. As the heat flux increased, the evaporation heat transfer coefficient increased. Regardless of the mass flux and saturation temperature, the smaller the tube diameter in the entire quality region, the higher the heat transfer coefficient was. Additionally, the average heat transfer coefficient of R-134a was observed to be higher than that of R-1234yf.

Keywords: R-1234yf, Evaporation, Heat transfer coefficient, HFO, Tube diameter

1. Introduction

In the 1930s, Freon-based refrigerants (CFCs and HCFCs), which have excellent efficiency and stability, were widely used in refrigeration and air-conditioning systems. However, if a Freon-based refrigerant leaks into the atmosphere, the ozone layer is destroyed by the chlorine component contained in these substances. Therefore, the use of CFC-based refrigerants has been completely banned since 2000, and HCFC-based refrigerants have also been after that, its use will be completely banned.

Recently, an alternative refrigerant that has been newly developed is R-1234yf, which is an HFO-based refrigerant. R-1234yf has similar thermal properties as R-134a, but it has a very low global warming potential; therefore, it has a very small environmental impact and is becoming popular as an alternative refrigerant for next-generation refrigeration and air-conditioning systems [1]. Various studies on the heat transfer properties of R-1234yf have been conducted [1]-[3], and

typical prior studies are outlined as follows.

Del Col *et al.* [3] measured the boiling heat transfer coefficient of R-1234yf in a circular microchannel with an inner diameter of 1 mm and compared it with that of R-134a. Lu *et al.* [4] studied the effect of heat flux and mass flux on the evaporation heat transfer coefficient of R-1234yf and R-134a in a horizontal tube with an inner diameter of 3.9 mm. Saitoh *et al.* [5] experimentally analyzed the evaporation heat transfer coefficient of R-1234yf in a horizontal tube with an inner diameter of 2 mm.

In summary, the research on the evaporation heat transfer of R-1234yf applied to refrigeration and air-conditioning systems has been conducted by many researchers, but it is still insufficient, and the theory of the heat transfer mechanism has not been established. Therefore, this study aimed to provide basic data on an R-1234yf evaporator by experimentally examining its heat transfer characteristics during the evaporation process for various horizontal diameters applied to the refrigeration and air-conditioning system.

[†] Corresponding Author (ORCID: <http://orcid.org/0000-0001-6375-2718>): Professor, Division of Energy facility, Korea Polytechnics University, 548, Kukwon-daero, Chungju-si, Chungcheongbuk-do 27324, Korea, E-mail: h0452@kopo.ac.kr, Tel: 043-850-4250

1 Professor, Department of Refrigerant and Air-Conditioning Engineering, Pukyong National University, E-mail: seolsh@pknu.ac.kr, Tel: 051-629-6184

2 Professor, Department of Refrigerant and Air-Conditioning Engineering, Pukyong National University, E-mail: yoonji@pknu.ac.kr, Tel: 051-629-6180

3 Ph. D., Department of Refrigerant and Air-Conditioning Engineering, Pukyong National University, E-mail: joonhyukcap3@naver.com, Tel: 051-629-6173

4 M. S., Department of Refrigerant and Air-Conditioning Engineering, Pukyong National University, E-mail: somy_03@naver.com, Tel: 051-629-6173

This is an Open Access article distributed under the terms of the Creative Commons Attribution Non-Commercial License (<http://creativecommons.org/licenses/by-nc/3.0>), which permits unrestricted non-commercial use, distribution, and reproduction in any medium, provided the original work is properly cited.

2. Experimental apparatus and method

2.1 Experimental apparatus

The experimental apparatus was designed to understand the heat transfer characteristics during the evaporation process of R-1234yf and to measure the evaporation heat transfer coefficient and pressure drop. **Figure 1** shows an overall schematic of the experimental apparatus, and **Figure 2** shows a detailed view of the evaporator. The evaporation test apparatus was composed of a magnetic gear pump, mass flow meter, preheater, heat transfer test section, receiver, auxiliary cooler, and thermostat. A magnetic gear pump was used to circulate R-1234yf in a supercooled state. The flow rate and density of the refrigerant were measured using a mass flow meter and the state of R-1234yf, which passed through the mass flow meter in a supercooled state, was checked.

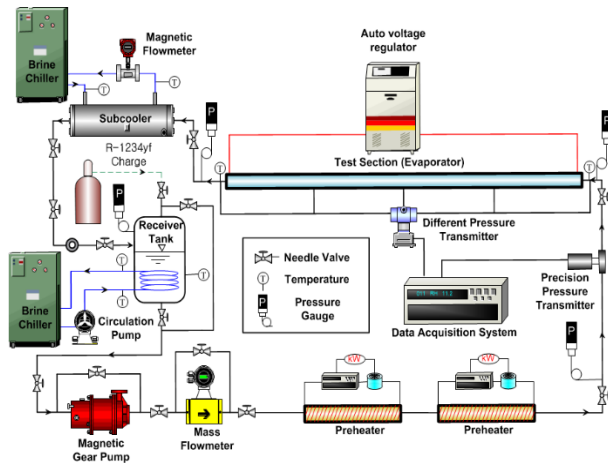


Figure 1: Schematic of experimental apparatus for evaporation heat transfer using R-1234yf

It is difficult to control the temperature and pressure simultaneously. Therefore, the saturation temperature was adjusted in a thermostat, and the quality and pressure were adjusted using a preheater before entering the test section. After the evaporation process in the test section, R-1234yf entered the auxiliary cooler for cooling and condensation. Because liquid and gas phases existed simultaneously in the receiver, the R-1234yf refrigerant liquid at the bottom was circulated by the magnetic gear pump. In addition, the low-temperature and low-pressure R-1234yf refrigerant liquid was circulated in the tube in the receiver to prevent phase change. In this study, these two methods were simultaneously applied to maintain the saturation temperature and quality suitable for the test conditions at the entrance to the test section.

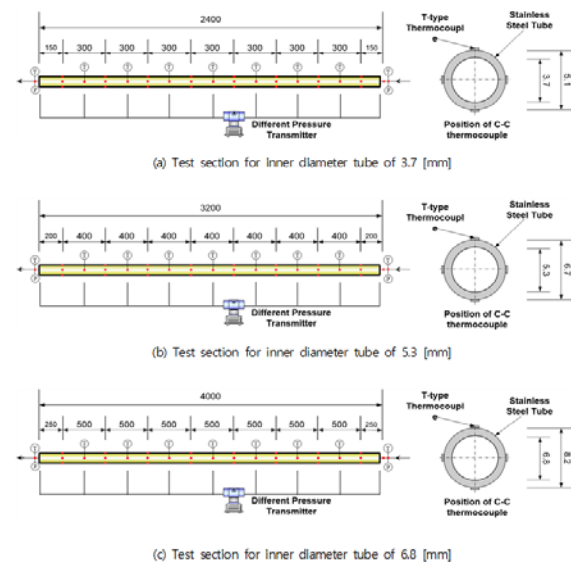


Figure 2: Schematic of test section for evaporation heat transfer with R-1234yf

In the experimental apparatus, the evaporation process could occur in the preheater and heat transfer test sections, and the preheater was divided into two preheaters to actively apply the energy required for phase change according to the mass flow rate. The evaporation test section was designed to control the amount of heat supplied using a variable voltage regulator. To control the quality of the refrigerant at the inlet of the test section, we designed the preheater to supply heat to R-1234yf by directly heating the stainless tube.

As shown in **Figure 2**, there were three types of evaporation test sections: 3.7, 5.3, and 6.8 mm stainless steel tubes; R-1234yf was heated using heat generated from a nichrome wire. Insulation fittings for high voltages were installed at both ends of the test section. The heating section was 2400 mm with an inner diameter of 3.7 mm, 3200 mm with an inner diameter of 5.3 mm, and 4000 mm with an inner diameter of 6.8 mm. A seamless tube was used to achieve a constant heat flux condition. To measure the temperature of the outer wall surface of the evaporator, we installed T-type thermocouples at the inlet and outlet of the evaporator at an interval of 300 mm for an inner diameter of 3.7 mm, an interval of 400 mm for an inner diameter of 5.3 mm, and an interval of 500 mm for an inner diameter of 6.8 mm. In addition, the middle of the evaporator was attached to the upper, lower, and side (left and right) four points at intervals of 300, 400, and 500 mm, respectively, and the temperature of the outer wall surface of the evaporator was measured. In addition, the refrigerant temperature was measured by inserting T-type thermocouples at intervals

of 300, 400, and 500 mm at the evaporator inlet. A pressure sensor and differential pressure gauge were installed at intervals of 300, 400, and 500 mm at the entrance to the test section to measure the pressure.

2.2 Experimental conditions and methods

Table 1 summarizes the experimental conditions of this study. R-1234yf, which passed the mass flow meter, was in a super-cooled state when the experimental device was operated normally. Here, while measuring the temperature and pressure of R-1234yf, we calculated the amount of heat required to pass through the preheater and become saturated using the refrigerant properties program REFPROP (Version 9.1) and then supplied it to the preheater to control the quality of R-1234yf.

$$Q_e = G_{re} \cdot i_{fg} \cdot x_{out} \quad (1)$$

where is Q_e is the amount of heat supplied to the test section, G_{re} is the mass flux of R-1234yf, and x_{out} is the quality adjusted in the preheater. When all of the above processes were completed, the pressure and temperature data were recorded and calculated in the test section.

2.3 Data reduction

The amount of heat exchange supplied to the outer wall of the stainless-steel tube through a hot wire and the amount of heat exchange gained by the R-1234yf flowing inside the tube were obtained to analyze the evaporation heat transfer characteristics. The heat flux supplied to the heating wire installed on the outer wall of the evaporator (q_e) was calculated using the following equation:

$$q_e = \frac{Q}{\pi \cdot d_i \cdot d_z} \quad (2)$$

where Q is the heat transfer amount, d_i is the average inner diameter, and d_z is the length of the subsection. Since the heat transfer coefficient in the circumferential direction of the tube has a significant influence on the performance of the system during

the evaporation process, it is necessary to calculate the heat transfer coefficient, which can be calculated using the following equation.

$$h_{e,loc} = \frac{q_e}{T_{e,w,in} - T_e} \quad (3)$$

Here, $h_{e,loc}$ represents the local heat transfer coefficient in the evaporator, T_e is the refrigerant temperature in the evaporator, and $T_{e,w,in}$ is the inner surface temperature of the tube wall in the evaporator. However, the inner surface temperature of the tube wall was calculated using the one-dimensional conduction equation at a steady state.

$$T_{e,w,in} = T_{e,w,out} - \frac{Q_{e,loc}}{2\pi \cdot k_w \cdot d_z} \cdot \ln\left(\frac{d_o}{d_i}\right) \quad (4)$$

Here, $T_{e,w,out}$ is the average wall temperature of the inner tube by averaging the surface temperatures of the upper, lower, and side portions of the tube, as shown in **Equation (5)**, and d_o and d_i are the outer and inner diameters of the inner tube, respectively. In addition, k_w is the thermal conductivity of the stainless tube.

$$T_{e,w,out} = \frac{T_{w,top} + 2T_{w,side} + T_{w,bottom}}{4} \quad (5)$$

Here, $T_{w,top}$, $T_{w,side}$, and $T_{w,bottom}$ are the measured temperatures of the upper, side, and lower wall surfaces of the inner tube, respectively.

Because the quality of the refrigerant can be calculated as in **Equation (6)**, the outlet quality ($x_{loc,out}$) of the subsection of the evaporator can be calculated using **Equation (7)**.

$$x = \frac{\Delta i_{loc}}{i_{lv}} \quad (6)$$

$$x_{loc,out} = x_{in} - \frac{\pi \cdot d_i}{M_e \cdot i_{lv}} \cdot \int_{z_{in}}^{z_{out}} q_e \cdot d_z \quad (7)$$

Here, Δi_{loc} is the refrigerant enthalpy difference at the entrance and exit of the subsection, and i_{lv} is the latent heat of the refrigerant. In addition, d_i is the inner diameter of the pipe and

Table 1: Experimental conditions for evaporation heat transfer

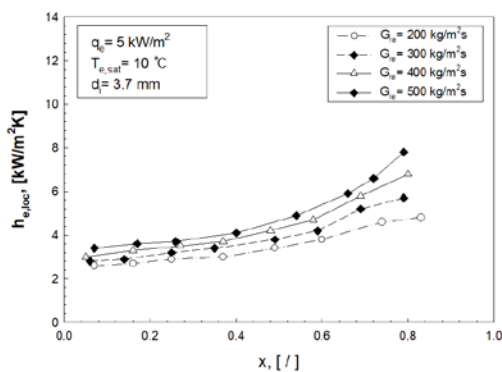
Refrigerant	R-1234yf		
Test section	Horizontal stainless steel		
Inner diameter of test tube [mm]	3.7	5.3	6.8
Heat flux [kW/m ²]	5, 10, 15		
Mass flux [kg/m ² s]	200 ~ 500		
Saturation temperature [°C]	5, 10, 15		
Quality [-]	0 ~ 1		

M_e is the refrigerant flow rate. In addition, z_{in} and z_{out} represent the inlet and outlet of the subsection, respectively, and q_e is the heat flux in the evaporator calculated using Equation (2), and $\pi \cdot d_i \int_{z_{in}}^{z_{out}} q_e dz$ is the accumulated heat quantity of the subsection from the heat exchanger inlet.

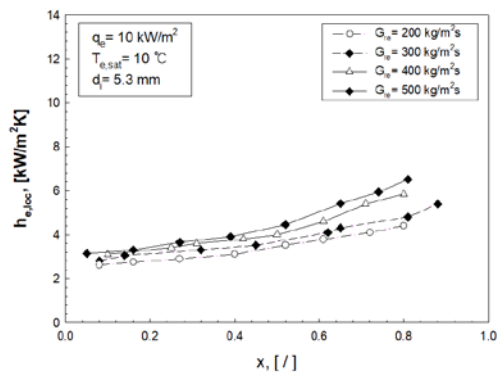
3. Experimental results and discussion

3.1 Effect of mass flux and quality

Figure 3 shows the local heat transfer coefficients according to the change in quality in tubes with inner diameters of 3.7 and 5.3 mm. As shown in the figure, as the quality increased, the local evaporation heat-transfer coefficient tended to increase. In particular, in the low-quality region, the heat transfer coefficient increased slightly as the quality increased. We considered that the porosity increased as the quality increased; thus, the thickness of the liquid film decreased; therefore, the evaporation heat transfer coefficient increased.



(a) $q_e = 5 \text{ kW/m}^2$, $T_{e,sat} = 10 \text{ }^\circ\text{C}$, $d_i = 3.7 \text{ mm}$



(b) $q_e = 10 \text{ kW/m}^2$, $T_{e,sat} = 10 \text{ }^\circ\text{C}$, $d_i = 5.3 \text{ mm}$

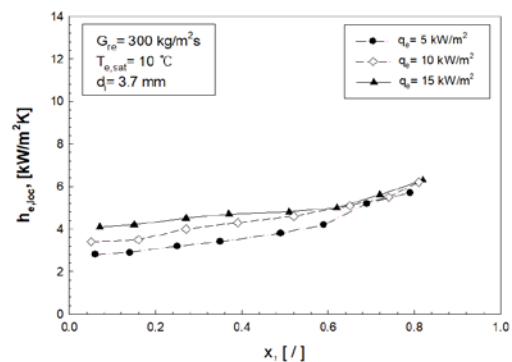
Figure 3: Variation in heat transfer coefficients for different mass fluxes at constant heat fluxes condition

Based on the local heat transfer coefficient of R-1234yf according to the change in the mass flux of the refrigerant under a

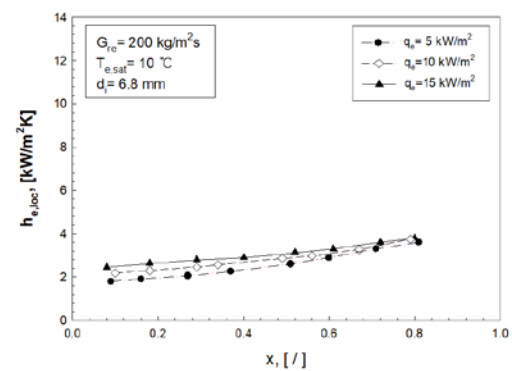
constant heat flux condition in Figure 3, the local heat transfer coefficient increased as the mass flux of R-1234yf increased in the entire quality region. This was considered to be because the Reynolds number (Re) increased when the mass flux of the refrigerant increased.

3.2 Effect of heat flux

Figure 4 shows the local evaporation heat transfer coefficient of R-1234yf with respect to the change in heat flux at a constant mass flux. As the heat flux increased, the local evaporation heat transfer coefficient increased, and this phenomenon was observed in the low-quality region. This meant that the nuclear boiling phenomenon that occurs only at low-quality regions also occurred at high-quality regions. That is, the heat transfer coefficient for the change in heat flux began to decrease as the steam quality increased further, meaning that convective boiling was suppressed in the high-quality region. Saitoh *et al.* [5] and Li *et al.* [6] also reported that the local heat transfer coefficient increased with an increase in the heat flux in the low-quality region under similar experimental conditions.



(a) $G = 300 \text{ kg/m}^2\text{s}$, $T_{e,sat} = 10 \text{ }^\circ\text{C}$, $d_i = 3.7 \text{ mm}$

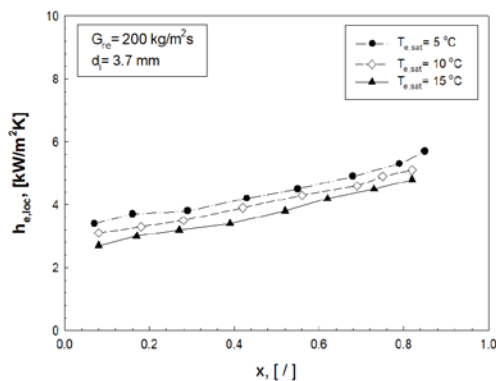


(b) $G = 200 \text{ kg/m}^2\text{s}$, $T_{e,sat} = 10 \text{ }^\circ\text{C}$, $d_i = 6.8 \text{ mm}$

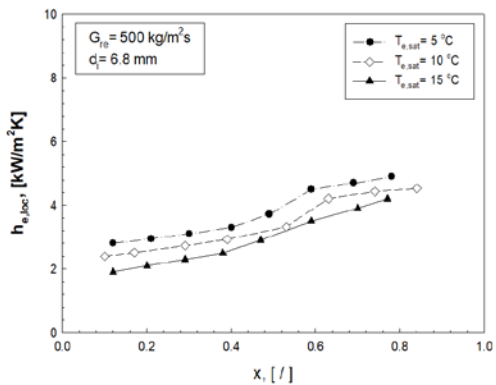
Figure 4: Variation in heat transfer coefficients for different heat fluxes at constant mass fluxes

3.3 Effect of saturation temperature

Figure 5 shows the local evaporation heat transfer coefficient according to the change in the saturation temperature of the refrigerant at a constant mass flux. The heat transfer coefficient decreased as the saturation temperature of the refrigerant increased. That is, in the nuclear boiling region, the bubble must escape from the tube wall. As the saturation temperature increased, the density ratio of the gas phase to the liquid phase decreased. Because of this, the buoyancy of the bubble decreased, the escape of the bubble was suppressed, and consequently, nuclear boiling was not activated. When the mass flux was different at a high saturation temperature, the evaporation heat transfer coefficient of the refrigerant was suppressed by the decrease in the buoyancy of the bubbles, and the evaporation heat transfer coefficient decreases. This trend was the same regardless of the change in the diameter. In contrast, an experimental study by Tong [7] indicated that the evaporation heat transfer coefficient increased owing to the enhancement of forced convective boiling in the high-quality region as the saturation temperature increased.



(a) $G = 200 \text{ kg/m}^2\text{s}$, $d_i = 3.7 \text{ mm}$

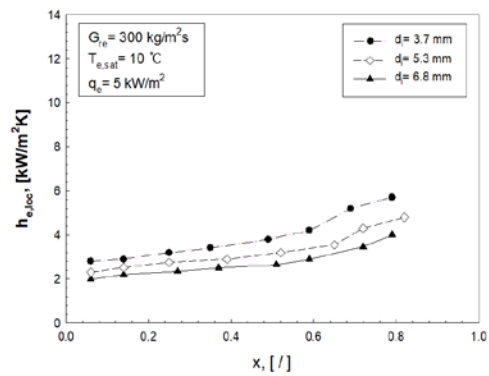


(b) $G = 500 \text{ kg/m}^2\text{s}$, $d_i = 6.8 \text{ mm}$

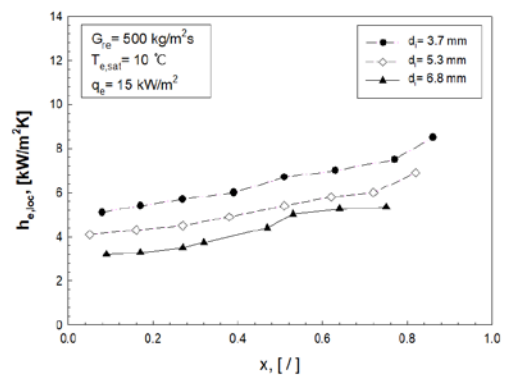
Figure 5: Variation in heat transfer coefficients for different saturation temperatures for constant heat and mass fluxes

3.4 Effect of change in tube diameter

Figure 6 shows the local heat transfer coefficient of R-1234yf with respect to the change in tube diameter under the same mass flux and saturation temperature conditions. We observed that the heat transfer coefficient increased as the diameter of the tube decreased in the entire vapor quality region regardless of the mass flux and saturation temperature. This was because the effective heat transfer area per unit volume of the refrigerant increased as the tube diameter decreased. In addition, as the diameter of the tube decreased, the refrigerant velocity increased; therefore, the annular flow dominated the low-vapor-quality region. Choi *et al.* [8] studied the evaporation heat transfer characteristics in three tubes with inner diameters of 3.1, 1.12, and 0.51 mm and observed the same results as above.



(a) $G = 300 \text{ kg/m}^2\text{s}$, $T_{e,\text{sat}} = 10 \text{ }^\circ\text{C}$, $q_e = 5 \text{ kW/m}^2$



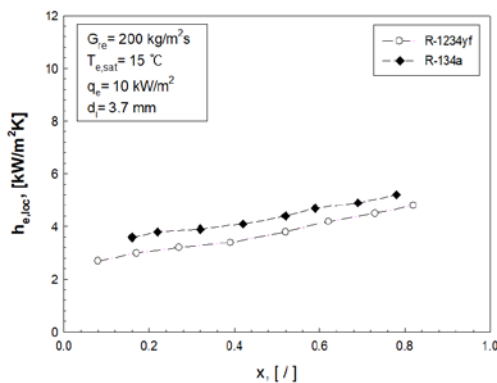
(b) $G = 500 \text{ kg/m}^2\text{s}$, $T_{e,\text{sat}} = 10 \text{ }^\circ\text{C}$, $q_e = 15 \text{ kW/m}^2$

Figure 6: Variation in heat transfer coefficients with different saturation temperatures for constant heat and mass fluxes

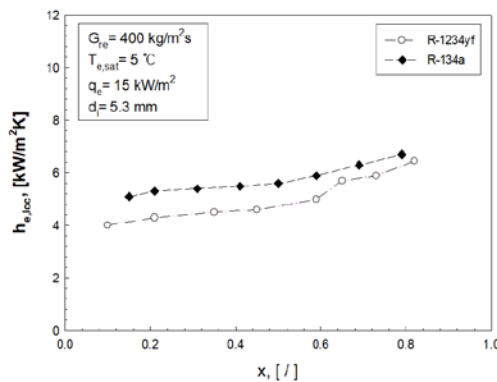
3.5 Compared with R-134a

Figure 7 compares the heat transfer coefficients of R-1234yf and R-134a. **Figure 7(a)** shows that when the mass flux is 200

kg/m²s, the heat transfer coefficient of R-134a is, on average, 16.2% higher than that of R-1234yf. **Figure 7(b)** shows that when the mass flux is 400 kg/m²s, the heat transfer coefficient of R-134a is, on average, 13% higher than that of R-1234yf. Thus, the heat transfer coefficient of R-1234yf is low in the entire vapor quality region because the density, latent heat, thermal conductivity, and surface tension of R-134a, a freon refrigerant, are higher in the gas phase. Saitoh *et al.* [5] and Li *et al.* [9] published the same results.



(a) $G = 200 \text{ kg/m}^2\text{s}$, $T_{e,sat} = 15 \text{ }^\circ\text{C}$, $q_e = 10 \text{ kW/m}^2$, $d_i = 3.7 \text{ mm}$



(b) $G = 400 \text{ kg/m}^2\text{s}$, $T_{e,sat} = 5 \text{ }^\circ\text{C}$, $q_e = 15 \text{ kW/m}^2$, $d_i = 5.3 \text{ mm}$

Figure 7: Comparison of heat transfer coefficients of R-1234yf and R-134a

4. Conclusions

In this study, the characteristics of evaporation heat transfer in a refrigeration/air-conditioning system using the refrigerant R-1234yf as the working fluid was investigated. Experiments were conducted using heat exchangers fabricated from tubes with inner diameters of 3.7, 5.3, and 6.8 mm, and the following conclusions, as a summary of the results, were obtained.

The evaporation heat transfer coefficient increased as the mass flux and heat flux of R-1234yf increased in the entire quality

region, and the evaporation heat transfer coefficient decreased as the saturation temperature increased. In addition, regardless of the mass flux and saturation temperature, the heat transfer coefficient increased as the tube diameter decreased in the entire quality region, and the average heat transfer coefficient of R-134a was observed to be higher than that of R-1234yf.

Author Contributions

Conceptualization, S. J. Ha; Methodology, S. J. Ha and J. H. Lee; Formal Analysis, H. S. Jeong; Investigation, S. J. Ha; Resources, S. J. Ha; Data Curation, S. J. Ha; Writing-Original Draft Preparation, S. J. Ha and J. H. Lee; Writing-Review & Editing, H. S. Jeong; Visualization, H. S. Jeong; Supervision, J. I Yoon and S. H. Seol; Project Administration, J. I Yoon and S. H. Seol.

References

- [1] K. Tanaka and Y. Higashi, "Thermodynamic properties of HFO-1234yf (2,3,3,3-tetrafluoropropene)," *International Journal of Refrigeration*, vol. 33, no. 3, pp. 474-479, 2010.
- [2] S. W. Lee, *Condensation Heat Transfer and Pressure Drop of HFO-1234yf in 4 mm Horizontal Tube*, M. S. Thesis, Graduate School of Refrigerant and Air-conditioning Engineering, Pukyong National University, Korea, 2021 (in Korean).
- [3] D. D. Col, S. Bortolin, D. Torresin, and A. Cavallini, "Flow boiling of R1234yf in a 1 mm diameter channel," *International Journal of Refrigeration*, vol. 36, no. 2, pp. 353-362, 2013.
- [4] M. -C. Lu, J. -R. Tong, and C. -C. Wang, "Investigation of the two-phase convective boiling of HFO-1234yf in a 3.9 mm diameter tube," *International Journal of Heat and Mass Transfer*, vol. 65, pp. 545-551, 2013.
- [5] S. Saitoh, C. Dang, Y. Nakamura, and E. Hihara, "Boiling heat transfer of HFO-1234yf flowing in a smooth small-diameter horizontal tube," *International Journal of Refrigeration*, vol. 34, no. 8, pp. 1846-1853, 2011.
- [6] M. Li, C. Dang, and E. Hihara, "Flow boiling heat transfer of HFO1234yf and R32 refrigerant mixtures in a smooth horizontal tube: Part I. Experimental investigation," *International Journal of Heat and Mass Transfer*, vol. 55, no. 13-14, pp. 3437-3446, 2012.
- [7] J. R. Tong, *Investigation of Convective Boiling Heat Transfer for Refrigerant R-134a and HFO-1234yf in a Smooth*

Tube, M. S. Thesis, Department of Mechanical Engineering, National Chiao Tung University, 2021 (in Chinese).

- [8] K. -I. Choi, J. -T. Oh, K. Saito, and J. S. Jeong, "Comparison of heat transfer coefficient during evaporation of natural refrigerants and R-1234yf in horizontal small tube," *International Journal of Refrigeration*, vol. 41, pp. 210-218, 2014.
- [9] Z. Li, H. Jiang, X. Chen, and K. Liang, "Evaporation heat transfer and pressure drop of low-gwp refrigerants in a horizontal tube," *International Journal of Heat and Mass Transfer*, vol. 148, p. 119-150, 2019.